



Cite this: *Chem. Commun.*, 2015, 51, 4985

Received 24th January 2015,  
Accepted 10th February 2015

DOI: 10.1039/c5cc00681c

www.rsc.org/chemcomm

## Rapidly assessing the activation conditions and porosity of metal–organic frameworks using thermogravimetric analysis†

Thomas M. McDonald, Eric D. Bloch and Jeffrey R. Long\*

**A methodology utilizing a thermogravimetric analyzer to monitor propane uptake following incremental increases of the temperature is demonstrated as a means of rapidly identifying porous materials and determining the optimum activation conditions of metal–organic frameworks.**

The gas adsorption properties of metal–organic frameworks are presently the subject of much investigation, owing mainly to their promise as gas storage and gas separation materials.<sup>1</sup> To accelerate the discovery of new adsorbents of this type, high-throughput robotics are sometimes utilized for screening synthetic conditions,<sup>2</sup> yet high-throughput methodologies for characterizing new phases are equally valuable.<sup>3</sup> Herein, we describe a rapid, convenient, and inexpensive methodology for assessing the activation conditions and porosity of metal–organic frameworks.<sup>4</sup> Utilizing a commercial thermogravimetric analyzer, the adsorption of propane at 50 °C proves to be a reliable probe of changes in adsorbent porosity. By comparing the relative quantities of propane adsorbed under different activation temperatures, a procedure for rapidly identifying the optimum activation conditions for metal–organic frameworks emerges.

Potential new metal–organic framework phases are generally first identified when solid products formed during a systematic survey of chemical space, typically dozens of reactions or more, are isolated and screened *via* powder X-ray diffraction.<sup>5</sup> In search of a characterization methodology that could augment X-ray diffraction by quickly distinguishing between nonporous and porous products, we sought to develop a procedure that addresses many of the challenges frequently encountered during the identification and activation of new solid adsorbents: (i) being accurate for small sample quantities (5 mg or less), (ii) requiring minimum effort from researchers to setup and analyze, and (iii) being inexpensive and widely transferable to the materials science community.

Towards these ends, our laboratory has recently begun to employ a modified thermogravimetric analysis (TGA) protocol for assessing the porosity of new reaction products.

In a typical experiment, a ~5 mg sample of the solvated metal–organic framework is heated under a flow of He gas at 50 °C min<sup>-1</sup> to 100 °C and held at that temperature for 15 min. The sample is cooled under a flow of He to 50 °C, at which point propane is isothermally introduced into the sample chamber. After 5 min, He is reintroduced across the sample and the solid is then heated to a higher activation temperature, usually 125 or 150 °C, for 5 min. Activation temperatures are incrementally increased, but propane adsorption is always measured at 50 °C to allow comparisons between different activation conditions. To illustrate the value of this methodology, data resulting from a traditional TGA experiment and the modified TGA experiment for a methanol-solvated metal–organic framework, Ni<sub>2</sub>(dobdc)·6MeOH (dobdc<sup>4-</sup> = 2,5-dioxido-1,4-benzenedicarboxylate; also known as Ni-MOF-74 or CPO-27-Ni),<sup>6</sup> are presented in Fig. 1.

In Fig. 1A, important but limited information about the material was obtained when it was heated to 600 °C under a flow of He. For example, the ~25% weight loss observed below 100 °C suggests that the material is likely porous. A second step observed around 275 °C, however, is less clear. It could signal the removal of bound methanol to metal cations, generating useful open metal sites,<sup>7</sup> or it could indicate the onset of framework decomposition. To establish definitively the thermal stability and activation conditions of the sample, which it has been amply demonstrated that the gas adsorption properties strongly depend upon,<sup>8</sup> multiple N<sub>2</sub> gas adsorption measurements at 77 K would be necessary. These measurements typically require 50–100 mg of sample each and a few days to complete, and therefore present significant hurdles for the high-throughput discovery of promising new adsorbents.

As shown in Fig. 1B, the modified TGA methodology quickly resolved the aforementioned uncertainties about activating the material. Again, solvent encapsulated within the pores was removed during the initial 15 min heating phase. The subsequent introduction of propane at 50 °C dramatically increased the mass of the sample owing to the adsorption of propane within the pores of

Department of Chemistry, University of California, Berkeley, CA 94720, USA.  
E-mail: jrlong@berkeley.edu

† Electronic supplementary information (ESI) available: Example TGA procedure and data analysis; additional CO<sub>2</sub> isotherms. See DOI: 10.1039/c5cc00681c

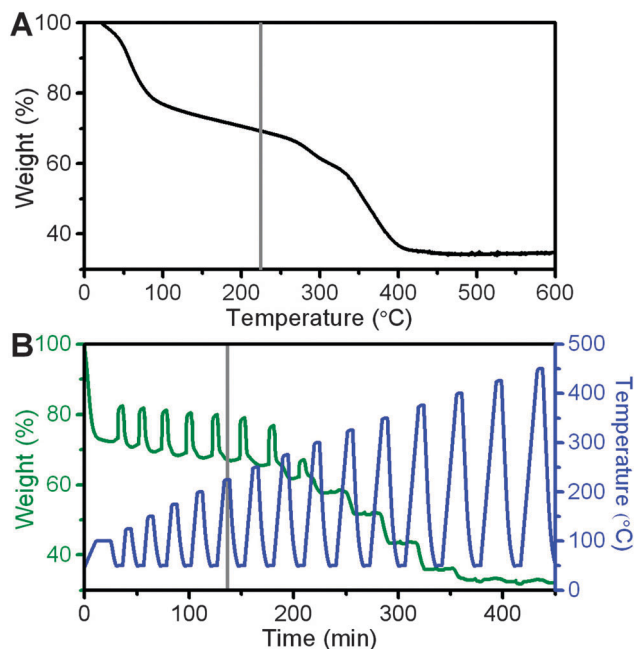


Fig. 1 (A) A traditional thermogravimetric analysis experiment performed on  $\text{Ni}_2(\text{dobdc})\cdot 6\text{MeOH}$  provides limited information about the optimal activation temperature. (B) The methodology presented here utilizes short heating cycles at high temperatures followed by the adsorption of propane at 50 °C as a probe for assessing the optimum activation conditions of metal–organic frameworks. The optimum activation temperature of 225 °C is highlighted as a vertical grey line in each plot.

the material. Upon reintroducing He, propane was quickly purged from the pores, and the sample mass returned to its baseline value. As the sample was activated at higher temperatures, small increases in the mass of propane adsorbed at 50 °C were observed until a maximum was achieved at 225 °C. Propane adsorption decreased slightly after activation at 250 °C, dramatically at 275 °C, and entirely after heating at 300 °C. From the results, it is clear that heating the solid even for short time to temperatures above 250 °C negatively affects the porosity of the adsorbent. If this metal–organic framework had actually been an unknown material, the modified TGA methodology would have established within 4 h and with only 3.8 mg of solvated solid that the material was porous and that the optimum activation temperature was between 200 and 250 °C. With activation steps of 50 °C, a survey of activation temperatures between 100 and 450 °C can be completed in approximately 3 h.

Additional surveys utilizing smaller step sizes or longer activation times over a narrower temperature range are helpful to further refine the activation conditions prior to scale-up. For scaled-up samples that are to be activated *in vacuo* rather than under a flowing gas, small differences in the optimum activation conditions may exist for some frameworks. Based upon our observations using this technique over the past 18 months, for frameworks where a discrepancy was observed, slightly lower temperatures could fully activate the adsorbent under high vacuum conditions.

The masses of propane adsorbed following activation at various temperatures between 100 and 450 °C are plotted in Fig. 2 for a selection of well-known metal–organic frameworks.<sup>9</sup> From this information, important data about the porosity, thermal stability,

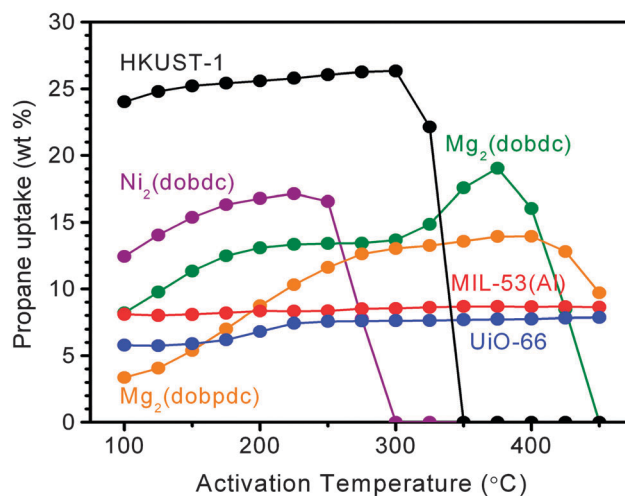


Fig. 2 The mass of propane adsorbed at 50 °C versus activation temperature is plotted for six well-known metal–organic frameworks.

and optimum activation temperature of materials can be readily obtained. For example, the technique would have quickly recognized that UiO-66<sup>10</sup> and MIL-53(Al)<sup>11</sup> possess exceptional thermal stability, since no decrease in the amount of propane adsorbed was apparent even after heating the samples to 450 °C. For UiO-66, an increase in the amount of propane adsorbed was observed as the material was heated between 200 and 250 °C. This increase likely corresponds to the reversible dehydration of the  $\text{Zr}_6$  cluster nodes that has been previously reported.<sup>12</sup> Remarkably, the small increases in surface area that result from dehydration are readily observable with this simple technique, even though other essential characterization methods, including powder X-ray diffraction, failed to capture the subtle event.

In comparison to  $\text{Ni}_2(\text{dobdc})$ , which rapidly loses porosity at temperatures above 250 °C,  $\text{Mg}_2(\text{dobdc})$ <sup>13</sup> exhibits excellent thermal stability for a metal–organic framework possessing open metal sites. With the short heating times and flow-through conditions used for the initial screen, higher activation temperatures than those typically reported for  $\text{Mg}_2(\text{dobdc})$  were found to be optimal. These high temperature, short duration activation conditions may prove valuable for activating large quantities of  $\text{Mg}_2(\text{dobdc})$  that contain strongly adsorbed species, such as methanol or water, which generally require many hours to be removed *in vacuo* at lower temperatures. Surprisingly, the pore expanded variant of  $\text{Mg}_2(\text{dobdc})$ ,  $\text{Mg}_2(\text{dobpdc})$  ( $\text{dobpdc}^{4-} = 4,4'$ -dioxidobiphenyl-3,3'-dicarboxylate),<sup>14</sup> exhibits slightly better thermal stability than the parent material, even retaining much of its porosity after being heated to 450 °C.

While some metal–organic frameworks, such as HKUST-1,<sup>15</sup> are tolerant to a large range of activation conditions, realizing the complete activation of metal–organic frameworks possessing open metal sites is particularly challenging, because framework decomposition often competes with metal site desolvation. For example,  $\text{Mn}_3[(\text{Mn}_4\text{Cl})_3(\text{BTT})_8(\text{MeOH})_{10}]_2$  ( $\text{Mn-BTT}$ ,  $\text{BTT}^{3-} = 1,3,5$ -benzenetris-tetrazolate),<sup>16</sup> was shown to exhibit promising  $\text{H}_2$  storage properties even though the majority of potential open metal sites remain ligated by methanol. To realize the previously reported  $\text{H}_2$  storage properties of Mn-BTT, activation conditions were surveyed utilizing

standard N<sub>2</sub> adsorption isotherms at 77 K over a two-month period of time in a process that required over 300 mg of sample to complete. Despite this careful survey, the best conditions were found to desolvate only ~17% of the potential open metal sites.

Improved activations conditions for Mn-BTT discovered by the methodology described here were realized with five experiments over a two-day period using just under 50 mg of solvated material. Activation of the framework under He for short periods of time at 180 °C was determined to be optimal based solely upon the amount of propane adsorbed at 50 °C (Fig. 3A). To validate these findings, excess CO<sub>2</sub> adsorption isotherms were collected for Mn-BTT activated using the previously reported activation conditions (150 °C, vacuum, 12 h) and the revised activation conditions (180 °C, flowing He, 1 h). As shown in Fig. 3B, 40% more CO<sub>2</sub> was adsorbed at 1 bar using the new activation conditions. Isostatic heat of adsorption calculations

(Fig. 3C) indicated an increase in the enthalpy of CO<sub>2</sub> adsorption of nearly 8 kJ mol<sup>-1</sup> at zero coverage. To the best of our knowledge, this is the third largest reported value for the differential enthalpy of CO<sub>2</sub> adsorption onto open metal sites in a metal-organic framework, falling just below the values of -63 kJ mol<sup>-1</sup> and -54 kJ mol<sup>-1</sup> measured for MIL-100(Cr) and MIL-100(V), respectively.<sup>17</sup> Furthermore, the activation of additional metal sites increases the number of CO<sub>2</sub> molecules that are strongly adsorbed; approximately 50% more CO<sub>2</sub> molecules are adsorbed with an enthalpy greater than 30 kJ mol<sup>-1</sup> with the revised activation conditions.

Although the methodology described here has been shown to be useful for a wide variety of framework structure types, it does have certain limitations. First, some metal-organic frameworks are unstable to traditional thermal activation methods, and for those materials this procedure would likely indicate that they are non-porous even though other methodologies, such as supercritical CO<sub>2</sub> drying, are capable of realizing their porosity.<sup>18</sup> Second, a smaller probe gas, namely CO<sub>2</sub>, would be more effective for assessing frameworks with small pores or pore windows.<sup>19</sup> While many researchers may find CO<sub>2</sub> to be superior to propane, the chemical inertness of propane and consistent heat of adsorption for different surface compositions makes it a better choice for our laboratory. For all surface chemistries, propane is quickly purged from the pores during subsequent heating steps. In addition, it is cheap, readily available, nontoxic, and convenient to use. No changes to the methodology are necessary if CO<sub>2</sub> is used in place of propane, and the effects of buoyancy discussed below apply equally.

For the purge gas, He, N<sub>2</sub>, and Ar were considered. For minimizing buoyancy effects, the fluid density of Ar most closely matches the density of propane, seemingly making it the most appropriate choice (Table 1).<sup>20</sup> However, when adsorbents were cooled under N<sub>2</sub> or Ar it became apparent that adsorption of the purge gas was significant enough to effect the calculated change in mass. Thus, despite the higher cost, He is the most suitable purge gas, since it obviates the need to account for purge gas adsorption. Furthermore, He is the most thermally conductive gas allowing short heating times to be utilized.

Owing to the large fluid density difference between He and propane, buoyancy effects should make samples appear lighter under propane than He. For nonporous materials, a decrease in sample mass is observed due to this effect. For this methodology, only samples that adsorb enough propane to overcome buoyancy effects will appear heavier under propane than He. As shown in Fig. 4, a simple visual inspection is sufficient to ascertain whether the sample mass increases or decreases, enabling a rapid differentiation between porous and nonporous materials. The ability of the technique to utilize very small samples masses to quickly identify

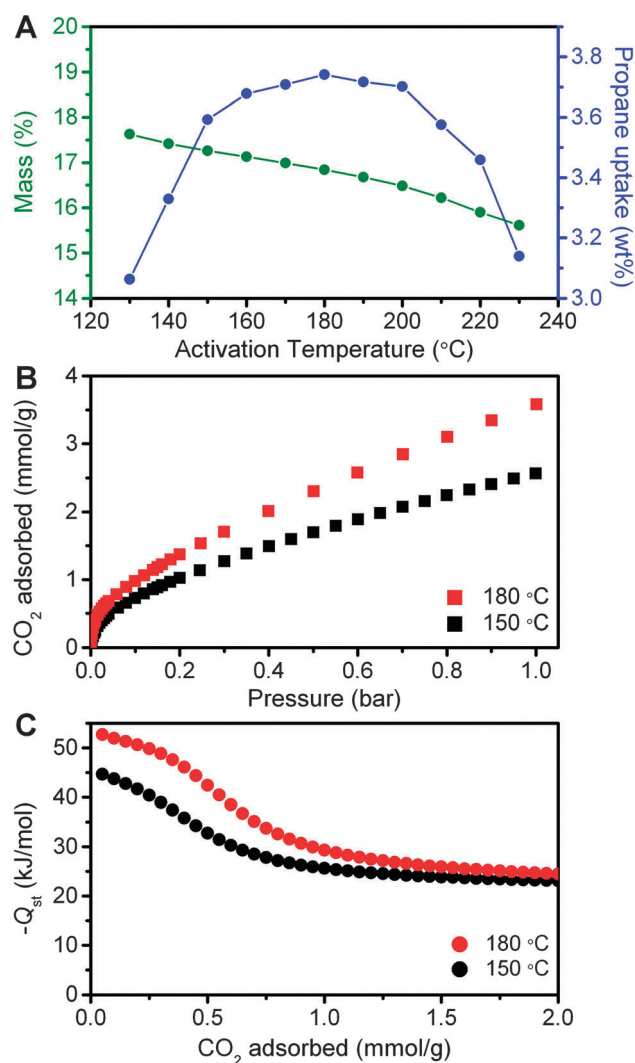


**Fig. 3** (A) While the mass of Mn-BTT shows a constant decrease with increasing activation temperature, the mass of propane adsorbed peaks after activation at 180 °C. (B) When compared to the originally reported activation conditions (150 °C), heating Mn-BTT at 180 °C for 1 h significantly increases the amount of CO<sub>2</sub> adsorbed at 25 °C. (C) The isosteric heat of CO<sub>2</sub> adsorption was observed to increase by 8 kJ mol<sup>-1</sup> at zero coverage using the 180 °C activation conditions reported here for Mn-BTT.

**Table 1** Thermophysical properties of gases at 50 °C and 1 atm

Gas	Density (mg mL <sup>-1</sup> ) <sup>20</sup>	Thermal conductivity (W m <sup>-1</sup> K <sup>-1</sup> ) <sup>20</sup>	Kinetic diameter (Å) <sup>19</sup>
He	0.1509	0.16420	2.6
C <sub>3</sub> H <sub>8</sub>	1.6840	0.02115	4.3
CO <sub>2</sub>	1.6661	0.01869	3.3
N <sub>2</sub>	1.0565	0.02739	3.64
Ar	1.5071	0.01884	3.40

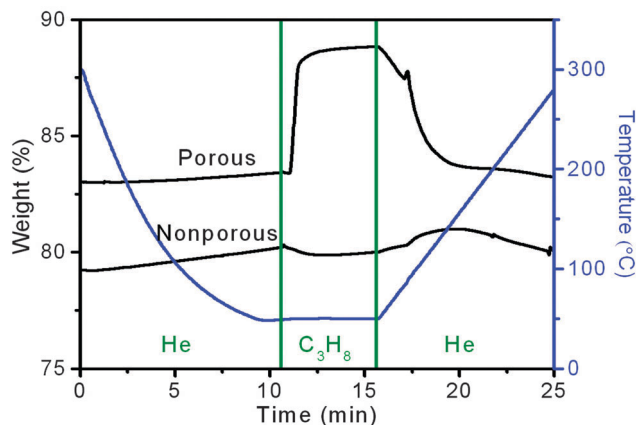


Fig. 4 Following activation at 300 °C, a porous and a nonporous material are cooled under He to 50 °C and exposed to propane for 5 min. Propane can adsorb within the pores of the porous material, causing the mass of the sample to increase. The mass of the nonporous sample appears to decrease due to buoyancy effects. Any increase in mass upon propane exposure is indicative of porosity, allowing porous and nonporous materials to be visually differentiated.

porous materials makes it a useful characterization technique for integration within protocols intended for the high-throughput discovery of new metal-organic framework adsorbents.

Because the change from He to propane is always effected under identical conditions, changes in buoyancy over time for any single experiment are negligible and comparisons between activation temperatures are possible without the need to account for buoyancy. Pore shape and functionalization significantly affect the quantity of propane adsorbed, and consequently no quantitative trend between adsorbent surface area and propane adsorption has been observed. Thus, definitive surface area comparisons among materials are still best made using traditional gas adsorption methods, since buoyancy effects must be accounted for if comparisons between different experiments using this technique are to be made.

Two benefits of this methodology differentiate it from a similar calorimetry-based instrument purpose-built for the high-throughput identification of porous metal-organic frameworks.<sup>3a</sup> First, most metal-organic framework researchers already utilize TGA instruments for routine sample characterization, so no new equipment purchase will be required for most researchers. Second, the calorimetric approach requires the preactivation of metal-organic framework samples, and thus is not capable of simultaneously identifying the proper activation conditions for the new materials.

With this technique, which is simple to perform, easy to analyze, and amenable to customization, we aim to provide a method that enables researchers and reviewers to determine whether the activation conditions reported for a metal-organic framework are in fact optimized. This may help prevent the publication of conflicting or incorrect gas adsorption data attributable to poor adsorbent activation. Further, the methodology is well suited for researchers utilizing high-throughput synthesis platforms or for those interested in developing metal-organic frameworks yet lacking the specialized

gas adsorption instrumentation necessary to differentiate porous from nonporous materials.

This research was funded by the Advanced Research Projects Agency-Energy (ARPA-E), U.S. Department of Energy, under Award Numbers DE-AR0000103 and DE-AR0000402.

## Notes and references

- (a) M. P. Suh, H. J. Park, T. K. Prasad and D.-W. Lim, *Chem. Rev.*, 2012, **112**, 782–835; (b) J. R. Li, J. Sculley and H.-C. Zhou, *Chem. Rev.*, 2012, **112**, 869–932.
- (a) R. Banerjee, A. Phan, C. Knobler, H. Furukawa, M. O’Keefe and O. M. Yaghi, *Science*, 2008, **319**, 939–943; (b) K. Sumida, S. Horike, S. S. Kaye, Z. R. Herm, W. L. Queen, C. M. Brown, F. Grandjean, G. J. Long, A. Dailly and J. R. Long, *Chem. Sci.*, 2010, **1**, 184–191; (c) M. Lammert, S. Bernt, F. Vermoortele, D. E. De Vos and N. Stock, *Inorg. Chem.*, 2013, **52**, 8521–8528.
- (a) P. Wollmann, M. Leistner, U. Stoeck, R. Grunker, K. Gedrich, N. Klein, O. Throl, W. Grähler, I. Senkowska, F. Dreisbach and S. Kaskel, *Chem. Commun.*, 2011, **47**, 5151–5153; (b) S. Han, Y. Huang, T. Watanabe, Y. Dai, K. S. Walton, S. Nair, D. S. Sholl and J. C. Meredith, *ACS Comb. Sci.*, 2012, **14**, 263–267; (c) P. Wollmann, M. Leistner, W. Grähler, O. Throl, F. Dreisbach and S. Kaskel, *Microporous Mesoporous Mater.*, 2012, **149**, 86–94; (d) J. J. Chen, X. Kong, K. Sumida, M. A. Manumpil, J. R. Long and J. A. Reimer, *Angew. Chem., Int. Ed.*, 2013, **52**, 12043–12046.
- J. E. Mondloch, O. Karagiardi, O. K. Farha and J. T. Hupp, *CrystEngComm*, 2013, **15**, 9258–9264.
- N. Stock, *Microporous Mesoporous Mater.*, 2010, **129**, 287–295.
- (a) N. L. Rosi, J. Kim, M. Eddaoudi, B. Chen, M. O’Keefe and O. M. Yaghi, *J. Am. Chem. Soc.*, 2005, **127**, 1504–1518; (b) P. D. C. Dietzel, B. Panella, M. Hirscher, R. Blom and H. Fjellvåg, *Chem. Commun.*, 2006, 959–961.
- (a) B. Chen, N. W. Ockwig, A. R. Millard, D. S. Contreras and O. M. Yaghi, *Angew. Chem., Int. Ed.*, 2005, **44**, 4745–4749; (b) L. J. Murray, M. Dincă, J. Yano, S. Chavan, S. Bordiga, C. M. Brown and J. R. Long, *J. Am. Chem. Soc.*, 2010, **132**, 7856–7857.
- S. J. Geier, J. A. Mason, E. D. Bloch, W. L. Queen, M. R. Hudson, C. M. Brown and J. R. Long, *Chem. Sci.*, 2013, **4**, 2054–2061.
- See ref. 6b, 10, 11, and 13–16, for the synthesis conditions of the metal-organic frameworks discussed here.
- J. H. Cavka, S. Jakobsen, U. Olsbye, N. Guillou, C. Lamberti, S. Bordiga and K. P. Lillerud, *J. Am. Chem. Soc.*, 2008, **130**, 13850–13851.
- T. Loiseau, C. Serre, C. Huguénard, G. Fink, F. Taulelle, M. Henry, T. Bataille and G. Férey, *Chem. – Eur. J.*, 2004, **10**, 1373–1382.
- L. Valenzano, B. Civalieri, S. Chavan, S. Bordiga, M. H. Nilsen, S. Jakobsen, K. P. Lillerud and C. Lamberti, *Chem. Mater.*, 2011, **23**, 1700–1718.
- S. Caskey, A. G. Wong-Foy and A. J. Matzger, *J. Am. Chem. Soc.*, 2008, **130**, 10870–10871.
- T. M. McDonald, W. R. Lee, J. A. Mason, B. M. Wiers, C. S. Hong and J. R. Long, *J. Am. Chem. Soc.*, 2012, **134**, 7056–7065.
- S. S.-Y. Chui, S. M.-F. Lo, J. P. H. Charmant, A. G. Orpen and I. D. Williams, *Science*, 1999, **283**, 1148–1150.
- M. Dincă, A. Dailly, Y. Liu, C. M. Brown, D. A. Neumann and J. R. Long, *J. Am. Chem. Soc.*, 2006, **128**, 16876–16883.
- (a) P. L. Llewellyn, S. Bourrelly, C. Serre, A. Vimont, M. Daturi, L. Hamon, G. De Weireld, J.-S. Chang, D.-Y. Hong, Y. K. Hwang, S. H. Jung and G. Férey, *Langmuir*, 2008, **24**, 7245–7250; (b) K. Sumida, D. L. Rogow, J. A. Mason, T. M. McDonald, E. D. Bloch, Z. R. Herm, T.-H. Bae and J. R. Long, *Chem. Rev.*, 2012, **112**, 724–781; (c) C. P. Cabello, P. Rumori and G. T. Palomino, *Microporous Mesoporous Mater.*, 2014, **190**, 234–239.
- A. P. Nelson, O. K. Farha, K. L. Mulfort and J. T. Hupp, *J. Am. Chem. Soc.*, 2009, **131**, 458–460.
- D. W. Breck, *Zeolite Molecular Sieves*, Wiley, New York, 1974, p. 636.
- National Institute of Standards and Technology. Thermophysical Properties of Fluid Systems. <http://webbook.nist.gov/chemistry/fluid/>, accessed May 09, 2014.